Revised 11 November 2004

The Thickness of Coastal Fast Ice in the Sea of Okhotsk

Kunio Shirasawa[1], Matti Leppäranta[2], Tuomo Saloranta[3], Toshiyuki Kawamura[4], Anatoli Polomoshnov[5] and Gennadi Surkov[5]

[1]Sea Ice Research Laboratory, Institute of Low Temperature Science, Hokkaido University, 6-4-10 Minamigaoka, Mombetsu, Hokkaido 094-0013 Japan;

[2]Division of Geophysics, University of Helsinki, Box 64 (Gustaf Hällströminkatu 2), FIN-00014 Helsinki, Finland;

[3]NIVA (Norsk institutt för vannforskning), Brekkeveien 19, Postboks 173, Kjelsås, N-0411 Oslo, Norway;

[4]Institute of Low Temperature Science, Hokkaido University, Kita-19, Nishi-8, Kita-Ku, Sapporo, Hokkaido 060-0819 Japan;

[5]Joint Stock Company "Sakhalin Projects", 18 Karl Marx St., Okha, Sakhalin 694460 Russia.

---

[1]e-mail kunio@pop.lowtem.hokudai.ac.jp, present address: Pan-Okhotsk Research Center, Institute of Low Temperature Science, Hokkaido University, Kita-19, Nishi-8, Kita-Ku, Sapporo, Hokkaido 060-0819 Japan

[2]e-mail matti.lepparanta@helsinki.fi, fax +358-9-19151000

[3]e-mail tuomo.saloranta@niva.no

[4]e-mail kawat@lowtem.hokudai.ac.jp

[5]e-mail ice@smng.com

[2]Corresponding author

Abstract

The thickness of coastal landfast ice in the Sea of Okhotsk has been examined based on field data and thermodynamic modelling. The study sites were Saroma-ko Lagoon, Hokkaido and Kleye Strait, Sakhalin. The ice sheet has a two-layer structure: a granular snow-ice layer on top and a columnar ice layer below. In Saroma-ko Lagoon the ice grows to 40–50 cm, with snow-ice portion of 10–100%. In Kleye Strait the ice grows to about 100 cm, with a remarkable addition (on average 24 cm) during mid-March to mid-April due to snow-ice formation. A one-dimensional thermodynamic ice–snow model was calibrated with observed data and used to examine the thickness climatology; the snow component takes into account snow compaction, slush formation due to flooding, melting or rain, and snow-ice growth. The model outcome showed reasonably good agreement for both sites. In Saroma-ko Lagoon the calibration was based on four winters. The maximum annual ice thickness was in the model on average 3 cm below the observed one, 16 cm in the worst case; the model snow thickness was within 10 cm from the observed ones in February; and the date of ice breakup was on average biased late by 5 days and 11 days in the worst case. The model simulations predicted formation of slush layers and their persistency for 1–4 weeks in different winters. Climatological simulation resulted in mean maximum annual ice thickness of 32 cm, of which 15 cm was snow-ice. In Kleye Strait the calibration was based on one ice season. The maximum annual ice thickness was 7 cm biased down, and the model snow thickness was within 10 cm from the observed level. Climatological simulation resulted in mean maximum annual ice thickness of 108 cm, of which 70 cm was congelation ice and 38 cm was snow-ice, and the ice season lasted from 5 November to 5 June. Thus slush formation and its freezing are crucial in the study basin.

Keywords Sea ice, snow-ice, slush, snow, thickness, mathematical modelling, oceanic heat flux, Sea of Okhotsk.

1. Introduction

The Sea of Okhotsk is a marginal sea of the northwest Pacific and belongs to the Seasonal Sea Ice Zone. It is located at latitudes of 44–59^{o} N and at longitudes of 135–155^{o} E, the surface area is 1.53x10^{6} km^{2}, and the mean depth is 838 m. There is a positive fresh water balance and consequently a two-layer structure with a strong halocline, which limits the vertical convection. The salinity is 32.5 psu (Practical Salinity Unit, 1 psu ≡ 10^{-3}) in the 50-m surface layer and 33–34 psu in the deeper layer. Every winter ice forms in the Sea of Okhotsk, and on average the maximum annual ice extent is 80% of the sea area and the length of the ice season is 5–6 months (e.g., Shirasawa, 1998).

The available observational sea ice data of the Sea of Okhotsk, mainly from Japanese and Russian literature, are very limited (e.g., Talley and Nagata, 1995). The thickness of thermally grown ice is from 30–60 cm at Hokkaido in the south up to 150 cm on the northern coast (Fig. 1). In recent years sea ice investigations have been increasing, much due to the exploitation of oil and gas offshore Sakhalin where sea ice information is needed for platform construction, for transportation of oil and gas, and for environmental risk analysis for oil spills (Anon., 2000). Research work in the Sea of Okhotsk has also been recommended to understand the ventilation of the North Pacific Ocean, including the formation of the North Pacific Intermediate Water where ice formation may play a significant role. One more aim has been to construct a realistic ice-ocean biogeochemical cycle model that enables us to predict annual and interannual key functions including the variability of the renewable resources (e.g., Talley and Nagata, 1995).

In a joint Japanese–Finnish research program "Ice Climatology in the Okhotsk and Baltic Seas", an experimental site was set up in the Saroma-ko Lagoon on the northern coast of Hokkaido for the growth, structure and properties, and decay of landfast ice (Shirasawa et al., 1996b). A similar site was established in Kleye Strait, Chaivo Bay off Sakhalin Island in a Japanese–Russian cooperative project “Sea Ice Studies off the Okhotsk Sea Coast of Sakhalin” (Shirasawa et al., 1996a). Both sites have provided very good data for the seasonal evolution of the ice conditions. An advanced model with snow metamorphosis and snow-ice formation, developed for the Baltic Sea (Saloranta, 2000), has been examined for its feasibility in the Sea of Okhotsk with good first results (Shirasawa et al., 1998; 2000).

Coastal landfast ice reflects the local winter climate, and its evolution is easily monitored together with the thermal forcing. The thickness of landfast ice is also a good reference for the thickness of undeformed drift ice further offshore, and it provides a good control for the thermodynamics of regional sea ice models.

In this paper the results of the structure and evolution of landfast ice in Saroma-ko Lagoon and Kleye Strait are presented. In particular the role of snow is analysed, including slush formation and snow-ice growth. The data are used to calibrate a thermodynamic snow–slush–snow-ice–congelation ice model with good success, and the model is utilized for analyses of the landfast ice climatology.

2. Ice Conditions and the Study Sites

2.1 Ice in the Sea of Okhotsk

Freezing in the Sea of Okhotsk normally begins in November on the northern coast. The maximum ice extent occurs in mid-March, and then the ice retreats disappearing by the beginning of June. The mean maximum annual thickness of landfast ice varies regionally within 30–150 cm (Fig. 1). On the coast of Sakhalin the ice grows to 70–120 cm, and the thinnest ice is found off Hokkaido, down to 30 cm (Fukutomi, 1952; Tabata et al., 1980). The thickness of drift ice varies largely due to mechanical processes. In the northern Sakhalin thicker pack ice floes are 120 cm thick (Polomoshnov, 1992), and off Hokkaido the thickness of undeformed drift ice is in the range of 19 to 55 cm (Shimoda et al., 1996).

Observations of the dates of freezing and breakup of sea ice started in 1892 by the Abashiri Observatory on the Hokkaido coast (Fig. 1). Daily visual observations of ice concentration within about 20 km from the coastline have been supplemented since 1930. The quantity "accumulated ice concentration", $A_T = \int_T A(t)\mathrm{d}t$, where A is ice concentration, t is time and T is the period from the freezing to breakup, has been used for the severity of the winters. It has decreased since 1930, while there has been an increasing trend in the annual mean air temperature (Aota et al., 1993). The average A_T has been 43.77 d, with the standard deviation 17.72 d and the range between 0.6 d in 1989 and 97 d in 1944 (Shirasawa and Leppäranta,

1996). Since 1969 a sea-ice radar network has been operative allowing continuous monitoring of ice field scenery along a 250-km northern coastline of Hokkaido to as far as 50 km offshore. The sea-ice coverage as observed by the radar network also shows a negative trend for the past years (Shirasawa, 1998). The length of the ice season in Abashiri has been recorded since the start-up of the ice radar system in 1969. The average and standard deviation are 17 January ± 10 days for the freezing date, 18 April ± 14 days for the breakup date, and 91 ± 18 days for the length of ice season during the period from 1969 to 2002.

2.2 Sites

Two specific landfast sea-ice sites are examined in this study: (1) Saroma-ko Lagoon, Hokkaido with maximum annual thickness of 30–60 cm, and (2) Kleye Strait, northern Sakhalin with maximum annual thickness of 70–120 cm. In both sites the ice is covered with snow, with significant amount of snow-ice formation as is typical for the whole Okhotsk Sea. These test sites were chosen to represent the ice conditions both in the southern and northern parts of the Sea of Okhotsk.

Saroma-ko Lagoon (Fig. 1) is 149.2 km^2 in area, 19.5 m in maximum depth, and 14.5 m in mean depth. Two main rivers provide Freshwater, and there are two inlets connected to the Sea of Okhotsk. About 90% of the total seawater inflow passes through the first (western) inlet opened in 1927, while the remainder comes via the eastern inlet built in 1978. The opening of the inlets has caused changes to the water mass and circulation of the lagoon. The salinity of the lagoon water is less than 32 psu, stratified in the ice season with low salinity levels beneath the ice. The ice site is in the eastern part of the basin, far from the main inlet.

Kleye Strait is 1–1.5 km wide and 15 m deep link between the Chaivo Bay and the Sea of Okhotsk (Fig. 1). Chaivo Bay is 40 km long and 5–7 km wide, and its water area is about 95 km^2. The salinity of the water varies between 10 and 30 psu due to tidal flows into and out from the Chaivo Bay. Shallow water regions with water depth of 0.5–1.0 m are rich in seaweed and occupy about 75% of the entire Chaivo Bay water area, and the diurnal tides are predominant with the maximum amplitude of about 2 m (Polomoshnov, 1994). In winter the water body freezes over for about 6 months.

3. Ice Thickness Climatology

3.1 Saroma-ko Lagoon

The average freezing date is 8 January, with remarkably small standard deviation (Table 1). In the beginning of the freeze-up, atmospheric forcing keeps the western lagoon open and frazil ice is formed there. This continues until the ice becomes more stable and the whole lagoon surface is covered with a level ice sheet. In five very mild recent winters (1989, 1991, 1993, 1997 and 2002) no full ice cover formed. The maximum annual thickness of ice is 35–60 cm in the eastern lagoon. On average, the growth to 34 cm takes one month, to mid-February, and thereafter the ice grows 8 cm more. There are spatial variations in ice thickness due to the heat flux from the first inlet leading to thinner ice in the western basin. In 1993 and 1997, when the western basin was open all winter, the thickness level was, however, as usual in the east.

The Saroma-ko ice sheet has a two-layer structure: a granular snow-ice layer on top and a columnar layer underneath. The bulk salinity of the ice has ranged through 1.5 to 5.1 psu in mid-winter, with higher values in the snow-ice layer due to the flooding of seawater in initiating the snow-ice formation. Recently ice structure analysis has commenced to investigate the detail structure of these layers (Kawamura et al., 2004). On average the columnar ice layer is 30% of the total thickness but variations are large, 0–82%, the rest being granular (average 23%) or granular/columnar (average 47%). The abundance of snow-ice is not surprising in considering the snow accumulation in the region. A few measurements of snow density are available for 2000–2002. The average density has been 0.24 Mg/m^3 on 15 February and 0.30 Mg/m^3 on 15 March.

At the Abashiri weather station the maximum annual snow thickness has averaged to 50.8 cm (standard deviation of 20.3 cm) while the average snow thickness on the ice in Saroma-ko has been 11 cm (standard deviation of 10 cm) in mid-February. The difference is partly explained by snow transport but much of it is in the snow-ice layer in the ice sheet. In the eastern basin no notable volume of frazil ice has been found, not even in 1997 when the western basin was ice-free all winter. A 40-cm snow layer could transform into a 10-cm snow-ice layer by melt–freeze cycles or into a 20-cm snow-ice layer by flooding.

In the five-year period 1992-1996 Saroma-ko lagoon froze over four times. The average date of full ice coverage was 3 February (standard deviation only 2 days), i.e. 26 days after the first ice formation. In the 1960s the timing of the full freeze-up was in mid-December, and a major shift occurred in 1979 corresponding to the opening of the second inlet (Shirasawa et al., 1998). In 1992–1996 the average breakup date of the full ice coverage was 12 April, with standard deviation of 6 days, while in 1963–1972 these numbers were 16 April and 7 days. The breakup date did not change much, because the spring heat budget is so strongly dominated by the incoming solar radiation.

There is a connection between the duration of full ice cover of Saroma-ko lagoon and the ice conditions within the 50-km radar coverage in Abashiri (Shirasawa et al., 1998). For the period 1979–2001, the correlation coefficient is 0.51 for the length of the ice season and 0.66 for the ice concentration integral A_T. Also in the cases with no full ice cover, the ice season on the Hokkaido coast was milder. Therefore the ice conditions in the lagoon can be used as an indicator for the ice climatology in the coastal region in the southern Okhotsk Sea.

3.2 Kleye Strait, Sakhalin

The ice season in Chaivo Bay starts from river mouths and lower salinity areas. The estimated average dates of freezing and breakup on the coast of northern Sakhalin are 25 November and 12 June during the period for 1935–1976. The ranges are 13 November – 15 December and 19 April – 6 July for the freezing and breakup, respectively. The length of the ice season is on average 200 days.

Also here the ice sheet consists of two layers: upper snow-ice layer and lower congelation ice layer. The bulk salinity of ice is in mid-winter usually 3–4 psu. In mid-December the average ice thickness in Kleye Strait is 38.5 cm, with the standard deviation of 9.8 cm (Table 2). The ice grows steadily by 0.5 cm/day during the next two months, then slowing down to reach 76-cm ice thickness in mid-March. The standard deviation stays at about 10 cm. Then a spring growth phase begins, and the maximum annual thickness is obtained in April, on average 100 cm and with a long-term maximum of about 120 cm. This spring growth is due to snow-ice formation and the resulting increase is drastic, an average of 24 cm added onto a 76 cm ice cover. Snow accumulation on the ice cover ranges between 10 and 55 cm. Melt water ponds

begin to appear at the beginning of April in the region, and a recurrent polynya forms in mid- or late April.

3.3 Analytical Modelling

In spite of their crudeness, simple analytic models provide rather good results for the climatology of sea ice thickness (Leppäranta, 1993). Denote thickness by h, density by ρ, thermal conductivity by κ, and temperature by T, with subscripts a for air, o for air–snow/ice interface, s for snow, si for snow-ice, i for normal sea ice, and w for water. The basic analytic model for congelation ice growth is based on the Stefan problem (Stefan, 1891). Thermal inertia and internal heating by solar radiation are ignored, and surface temperature $T_o = T_o(t)$ is prescribed. A generalized form including a practical modification, due to that normally the surface temperature must be estimated from the air temperature T_a, reads in differential form

$$\frac{\mathrm{d}h_i}{\mathrm{d}t} = \frac{a}{2} \times \frac{T_f - \min\{T_a, T_f\}}{h_i + d} - \frac{Q_w}{\rho_i L} \tag{1}$$

where t is time, $a = 2\kappa_i/\rho_i L$, L is latent heat of freezing, T_f is freezing point temperature, d is the effective insulating thickness of the near surface air – snow buffer, and Q_w is the oceanic heat flux. Stefan's solution $h_i = \sqrt{aS}$, where $S = \int_o^t (T_f - \min\{T_a, T_f\})\mathrm{d}t'$, comes from $d = Q_w = 0$ and can be taken as an upper bound for favourable ice growth conditions. With $Q_w = 0$ the Zubov's (1945) solution is obtained: $h_i = \sqrt{aS + d^2} - d$; with $Q_w \neq 0$ and T_a = constant < T_f, there is a steady-state solution $h_i = \max\{\kappa_i(T_f - T_a)/Q_w - d, 0\}$.

Snow-ice grows from the top of the slush, and the growth equation is (Leppäranta, 1993)

$$\nu \frac{\mathrm{d}h_{si}}{\mathrm{d}t} = \frac{a}{2} \times \frac{T_f - T_s}{h'_{si}} = \frac{\kappa_s}{\rho_i L} \times \frac{T_s - T_a}{h_s} \tag{2}$$

where ν is the water fraction of the slush layer, h'_{is} is the thickness of snow-ice above the slush, and T_s is the surface temperature of snow-ice. Note that h'_{is} is used instead of h_{si} in the centre term because only the part of snow-ice, which is above the freezing slush, counts for

insulation. If $h_{is}^{'} \equiv 0$, new slush form continuously and the upper limit of snow-ice thickness is obtained. Then, in the case of flooding $h_s = \gamma h_{si}$, where $\gamma = (\rho_w - \rho_i)/\rho_s$, and

$$\frac{\mathrm{d}h_{si}}{\mathrm{d}t} = a_{si} \times \frac{T_f - T_a}{h_{si}} \tag{3}$$

where $a_{si} = (\gamma/\nu)^{1/2} a$. Taking $\gamma \approx 1/3$ and $\nu \approx 1/2$ (Leppäranta and Kosloff, 2000), the factor $(\gamma/\nu)^{1/2}$ becomes 0.8. Thus snow-ice formation by flooding is limited by snow insulation. In the case of snow-ice formation from meltwater or liquid precipitation, the principal limiting factors are how much latent heat can be taken out of the slush and how much liquid water is in the slush.

Abashiri meteorological station data give annual freezing-degree-days of 300–400 ^{o}C·day. The pure Stefan's law would give estimates of 57–66 cm for the maximum annual ice thickness, about 10–20 cm more than in reality. In Saroma-ko lagoon snow-ice growth dominates, and the pure top growth law (Eq. 3) brings the thickness range down to 46–53 cm, which includes the annual observed average maximum ice thickness. The oceanic heat flux is therefore small in the eastern basin. According to an analytical model (Leppäranta et al., 1997), Q_w ~10 W/m^2 would drop the annual maximum thickness down by ~10 cm in Saroma-ko conditions, which would be too much in the light of the observed data.

In Kleye Strait the ice is mostly snow-covered congelation ice. In 1990–1995 the sum of the freezing-degree-days was on average 1350 ^{o}C·day, with standard deviation of 300 ^{o}C·day. Zubov's (1945) formula with empirical parameters a = 8 cm^2/(^{o}C·day) and d = 25 cm provides a good fit with observations of ice growth. The mean freezing-degree-days yields an ice thickness of 82 cm while the mean observed ice thickness is 76 cm in mid-March but as much as 100 cm in mid-April (Table 2). The Stefan's law for the growth of bare congelation ice would give an estimate of 122 cm for the maximum annual ice thickness.

The snow-ice formation in spring is due to flooding and/or melt-freeze cycle. Assume that there is initially a snow cover of thickness h_{so}. If a slush layer of thickness h_{sh} is formed in the lower part, it will freeze into snow-ice according to Eq. (2) with $h_s = h_{so} - h_{sh}$ = constant, and the solution is of Zubov form, $h_{is}^{'} = \sqrt{\nu^{-1} aS + d^2} - d$, where $d = (k_i/k_s)h_s$ is the insulating

effect of snow. If $S \sim 200$ °C·day for a spring month, then $d \sim 100$ cm would give $h_{is}' \sim 20$ cm. Such S levels exist in our April data. The slush layer formation by flooding necessitates $h_{so} \sim 50$ cm, and then we would need $(k_i/k_s) \sim 5$, which is possible for dense snow. Snow density measurements have given 0.375 Mg/cm^3, which gives $k_i/k_s \approx 5.9$ (Yen, 1981; see next chapter). Snow-ice formation from melt-freeze cycles is easier since then the insulating effect of snow becomes reduced; also then the initial snow thickness needs to be around 50 cm and $S \sim 100$ °C·day would be enough.

4. Numerical Modelling of Ice Thickness

4.1 Model Description

A snow/sea-ice thermodynamic model, earlier developed for the Baltic Sea (Saloranta, 1998, 2000) is employed in the present work. It consists of the classical Maykut and Untersteiner (1971) model and a snow model, which takes account of snow compaction, slush formation from flooding, melting or rain, and snow-ice growth (Fig. 2). The basic equation is the classical 1-d (vertical) heat conduction equation:

$$\frac{\partial \rho c_i T}{\partial t} = \frac{\partial}{\partial z}\left(\kappa \frac{\partial T}{\partial z} - I \right) \tag{4}$$

where c_i is specific heat of ice, and I is solar radiation penetrating into the snow and ice. The boundary conditions come from the continuity of heat flux with a moving top and bottom boundaries:

Top:
$$\kappa \frac{\partial T}{\partial z} = \rho L \frac{\mathrm{d}h}{\mathrm{d}t} + Q_o , \tag{5a}$$

$$\frac{\mathrm{d}\, h_s}{\mathrm{d}t} = P - S - M - C \tag{5b}$$

Ice/Snow interface:
$$\kappa \frac{\partial T}{\partial z} = \kappa_s \frac{\partial T}{\partial z}, \text{ if } h_{sh} = 0 \tag{6a}$$

$$\rho_{si} L v \frac{\mathrm{d}\, h_{si}}{\mathrm{d}t} = \kappa_s \frac{\partial T}{\partial z} - \kappa \frac{\partial T}{\partial z}, \text{ if } h_{sh} > 0 \tag{6b}$$

$$\frac{\mathrm{d}\,h_{sh}}{\mathrm{d}t} = S \tag{6c}$$

Bottom: $$T = T_{\mathrm{f}}\,, \tag{7a}$$

$$\rho_i L \frac{\mathrm{d}\,h_i}{\mathrm{d}t} = \kappa \left.\frac{\partial T}{\partial z}\right|_{bottom} - Q_w \tag{7b}$$

where Q_o is the top surface heat balance, P is snowfall rate, S is slush formation rate, M is snow-melting rate, C is snow compaction rate, and h_{sh} is the thickness of slush layer. The term Q_o includes the radiation balance and turbulent heat exchange with the atmosphere.

The thickness of snow increases due to snowfall, given as the water equivalent into the model and changed to snow thickness using a fixed density of new snow. The threshold value between snow and no-snow conditions in the model is set to 3 cm. The thickness of snow decreases due to three different reasons: surface melting, compaction, and transformation to slush. The density change in snow due to compaction is formulated after Yen (1981) as

$$\frac{\partial \rho_s}{\partial t} = \rho_s C_1 W_s \exp(-C_2 \rho_s) \exp[-\frac{(T_f - T_a)}{12.5°C}] \tag{8}$$

where $C_1 = 7.0\ \mathrm{m^{-1}\,h^{-1}}$ and $C_2 = 21.0\ \mathrm{Mg^{-1}\,m^3}$ are empirical coefficients, and W_s is the volume of overlaying snow in equivalent thickness of water. A depth dependent snow density profile due to snow compaction was calculated. An upper limit of 0.45 $\mathrm{Mg/m^3}$ is assumed for the snow density (Leppäranta, 1983).

The density of the water-soaked snow in slush formation is assumed to rise to 0.45 $\mathrm{Mg/m^3}$. If negative freeboard conditions appear, the amount of new slush is calculated from

$$\frac{\partial H_{sh}}{\partial t} = \frac{1}{(\rho_s + \rho_w - \rho_{sh})} \frac{\partial (\rho_{fw} W_s - B)}{\partial t} \tag{9a}$$

$$B = h_{\mathrm{i}}(\rho_{\mathrm{w}} - \rho_{\mathrm{i}}) + h_{\mathrm{si}}(\rho_{\mathrm{w}} - \rho_{\mathrm{si}}) + h_{\mathrm{sh}}(\rho_{\mathrm{w}} - \rho_{\mathrm{sh}}) \tag{9b}$$

where ρ_{fw} is density of pure water, and B is the buoyancy of ice, snow-ice and old slush layers. In the model a fixed snow overload is needed for the flooding event to begin; here it is taken

as 3 mm of water equivalent. The thermal conductivity of snow is formulated after Yen (1981) as $\kappa_s = 2.22362(\rho_s)^{1.885}$, where κ_s is in W/(m°C) and ρ_s is in Mg/m^3.

The snow-ice growth model was first given in a three-layer model of Leppäranta (1983) initiated from flooding of seawater. It was further used by several authors, as applied by Fritsen et al. (1998) for microalgal dynamics. Saloranta (2000) presented a fine resolution sea ice model with snow-ice formation allowed also from melt-freeze cycles in snow cover and liquid precipitation, while Maksym and Jeffries (2000) examined a coupled temperature-salinity model of sea ice and suggested upward brine flows as an additional mechanism to produce slush on the top surface of sea ice.

The surface heat budget is written as

$$Q_o = Q_r + Q_L + Q_h + Q_e \tag{10}$$

where Q_r is net shortwave radiation, Q_L is net long-wave radiation, Q_h is turbulent sensible heat flux, and Q_e is turbulent latent heat flux. The bulk formulae have been used for the turbulent fluxes with the transfer coefficients of $1.75 \cdot 10^{-3}$ (Crocker and Wadhams, 1989) while the radiation terms are

$$Q_r = (1-\alpha)(1-i_o)\tau f(N)\, Q_s \tag{11a}$$

$$Q_L = \varepsilon\sigma[\underline{T}_a^4(A+Be^{1/2})(1+CN^2) - \underline{T}_o^4] \tag{11b}$$

where α is albedo, i_o is the part of the solar radiation penetrating the surface, τ is atmospheric turbidity, f is a correction factor depending on the cloudiness N (Reed, 1977), Q_s is the solar radiation on a horizontal surface on top of the atmosphere, ε is emissivity of the ice/snow surface, σ is Stefan-Boltzmann constant, A = 0.68, B = 0.0036 mb$^{-1/2}$ and C = 0.18 are empirical parameters, e is water vapour pressure, and the underlined temperatures refer to the absolute temperatures. The formulation of the long-wave radiation is as in Omstedt (1990). Snow and ice albedos were defined separately for four different surface conditions. The model parameters and constants are given in Table 3.

The model is forced by local data for the calibration. Climatological ice and snow simulations are then performed with local weather data for Saroma-ko Lagoon, but for Kleye Strait such long-term record does not exist and instead the NCEP/NCAR reanalysis data are used (http://www.cdc.noaa.gov/). The sea-ice growth modelling problem possesses a negative feedback to errors, which makes it relatively easy. Also the thicker the ice grows, the less is the thickness sensitive to atmospheric forcing. Indeed, the background Stefan's law tells that squared ice thickness is proportional to the freezing-degree-days S (see section 3.3), and consequently $\delta h_i \propto \delta S/h_i$. With snow accumulation, snow metamorphosis, slush formation, and snow-ice growth, the sensitivity to the treatment of snow steps into the picture, and the model outcome may lead to large persistent deviations (see Leppäranta, 1983).

4.2 Saroma-ko Lagoon

Meteorological forcing data were available for 1987–1996 at six-hour time interval at Abashiri Observatory (Sapporo District Meteorological Observatory, 1987–1996), located a bit southeast from the study site (Fig. 1). Snow and ice thickness measurements were made at a fixed site apart about 1 km from the southeast coast of the lagoon. The standard oceanic heat flux was set to 5 W/m^2 corresponding to measurements at the site, and for sensitivity analysis the low and high levels were taken as 0 and 20 W/m^2. The density of new snow was set to 0.225 Mg/m^3 (close to observed level in mid-February), the sea surface salinity to 31.5 psu, and the model time-step to 1 h. The starting time of the model was taken as the observed date of freezing, and ice formation began then as soon as the net heat flux became negative. Results from the modelled Saroma-ko lagoon ice winters are shown in Fig. 3 and Table 4.

In winter 1992 the modelled maximum ice thickness was 26 cm and the day of breakup was 6 April. This year's model fit was the worst. The ice was mainly congelation ice, with steady growth until 25 March. Observed ice thickness was 33–42 cm from 22 February to 20 March (Shirasawa et al., 1997), consistently higher than the modelled maximum. The observed snow thickness showed variability with likely loss due to snow-ice formation in late February. The modelled day of breakup showed a fairly good consistency with the observed day of 4 April.

In winter 1994 the site froze at the beginning of January and first the congelation ice growth was dominant in the model. Two persistent slush layer periods occurred: 20 February – 5 March and 20 March – 10 April. The ice thickness was at its maximum at the beginning of

April, and the snow-ice fraction increased to more than 50% during the snow-melting period. On 28 February the observed snow and ice thicknesses were of 9 cm and 38 cm, respectively, as given by the model (see Fig. 3). The modelled breakup day (21 April) showed a good agreement with the observed day of 17 April (Table 4).

In winter 1995 ice formed at the beginning of January, and one month later the ice thickness was 25 cm. A thick slush layer formed in mid-February and remained on ice for four weeks. At the beginning of March the ice thickness reached its maximum of 45 cm, in agreement with observations, and the snow-ice fraction became large due to bottom melting of the congelation ice. There was a little less snow in the model than in the observed data (Fig. 3; note that the slush layer must be added to the model snow line). The modelled day of breakup on 12 April showed a good consistency with the observed day of 10 April.

Winter 1996 was reproduced well by the model. The model ice was almost all congelation ice, and only in the spring melting season significant snow-ice layer formed. The modelled maximum ice thickness was 39 cm, while the observed values were 33–36 cm. Also the modelled snow thickness (5–15 cm) was consistent with observations (7–9 cm). The modelled day of breakup on 27 April was 11 days delayed from the observed 16 April, the error being larger than in other years.

In all, the model outcome shows a two-layer ice structure with a snow-ice layer on top and a congelation layer below, and the relative proportions of these layers vary largely from year to year. In 1992 the ice was mainly congelation ice, while in 1995 the snowfall was heavy from mid-February to mid-March, and the consequent slush/snow-ice formation turned gradually most of the ice sheet into snow-ice. A slush layer was found every winter, and except for 1992 this layer persisted several weeks. Most of the snow-ice was due to infiltration of seawater into the snow due to the weight of snow, while a small addition comes in the snow-melting season due to the diurnal cycle in the surface heat budget. Ice thickness and ice break-up date were predicted fairly well by the model, with the mean errors of 3 cm and 5 days (Table 4). In 1992 the error in ice thickness was 16 cm and in 1996 the error in the break-up date was as large as 11 days. The two-layer structure of the ice sheet as well as the large year-to-year variability of the thicknesses of the layers corresponds well to observations. In the present model the ice melts where it is, but in reality the ice breaks and drifts before the final melting. Due to this breakage the ice disappears a few days earlier than otherwise.

The 10-year period 1987–1996 was then taken for a climatological simulation. Three winters when the lagoon did not completely freeze over were excluded from the calculations. The resulting mean evolution of the thicknesses of snow (including slush), snow-ice and congelation ice averaged over the seven winters is shown in Fig. 4. First the congelation ice growth is dominant, and in the beginning of February the ice thickness is 20 cm. A month later it is 27 cm, and in March the growth is mainly due to snow-ice formation. The maximum ice thickness is 32 cm, 10 cm less than observed in 1992–1996 (the shorter observation period partly explains the difference: for these years the mean bias down was only 3 cm in the model.). At the time of the thickness maximum the snow-ice thickness is 15 cm, and the snow-ice fraction increases to more than 50% during the melting period. The ice breakup date is 20 April, eight days later than the observed average date.

The snow metamorphosis and the oceanic heat flux are the crucial model elements. The fact that the modelled snow thickness agrees rather with the measurements, both in the case years and in the statistics, suggests that relevant snow physics are now rather well represented. The oceanic heat flux corresponds to a typical level but its temporal variations are not included. Its role was examined with a sensitivity analysis (Fig. 5). When the oceanic heat flux is zero, the maximum ice thickness becomes 42 cm, 10 cm more than in the standard case (5 W/m^2). The snow-ice thickness is about the same (15 cm) in absolute units but less relatively speaking. When the oceanic heat flux goes to 20 W/m^2, the ice thickness is 18 cm at maximum and it is almost all snow-ice. Congelation ice is formed in the early ice season but it is melted by the oceanic heat flux, while snow-ice continues to grow. Thus also the proportions between congelation ice and snow-ice are largely affected by the oceanic heat flux. The snow-ice layer extending down through the ice sheet due to the melting of congelation ice was also reported by Lytle and Ackley (2001) in the Weddell Sea.

Since the snow layer thickness was realistic in the model, it is interesting to look further into the predicted snow layer (Fig. 6). The density of snow increases from the initial level of 0.225 Mg/m^3 to 0.3 Mg/m^3 in March and to about 0.35 Mg/m^3 in April. The evolution for February–March is as the existing observations (see section 3.1) but for April no data exist to compare. An average 2–4 cm slush layer is on top of the ice for 40 days from late February to the beginning of April. The slush layer thicknesses have not been recorded, but observations typically show for the lower part of the snow layer high salinities, which is an indication of

the presence of slush. The slush layer is important for controlling the surface temperature of the ice and thus the temperature of the whole ice and snow sheet. Also a persistent slush layer opens possibilities for algae growth at the ice–snow interface.

4.3 Kleye Strait

Meteorological observations have been collected at Chaivo Research Station (Fig. 1) near the shore of Kleye Strait, which links Chaivo Bay to the Sea of Okhotsk (Shirasawa et al., 1996a). The data for the ice season 1994/1995 are used for the model calibration. Short-wave radiation flux was calculated from the measured total daily solar insolation assuming the flux to vary sinusoidally between sunrise and sunset. An average value for cloudiness (55%) was taken from Peixoto and Oort (1992; p. 173–175). The density of new snow was 0.25 Mg/m^3, the sea surface salinity was 4.0 psu, and the model time-step was 2 h. The standard oceanic heat flux was fixed to 10 W/m^2. Ice and snow observations were available for 29 December 1994 – 22 April 1995 (Shirasawa et al., 1996a), and the calibration run was consequently initialised in 29 December. Precipitation rate was averaged from snow thickness and density observations and kept constant at 1.56 mm water equivalent/day during the ice season.

The total ice thickness was well reproduced by the model, within 10 cm (Fig. 7). At the end of the observation period the model ice thickness was 88 cm while the observed value was 95 cm. Snow-ice formation began on 15 February and continued then the whole time, and at the same time congelation ice growth ceased and its thickness began to decrease slowly. The temperature at the ice–snow interface was very well reproduced by the model (Fig. 7), strongly supporting the quality of the modelled heat fluxes. The oscillations in the modelled curve in the later period are due to the model threshold value of 3 mm water equivalent of snow overload needed for the flooding event.

The constant precipitation rate in the model produced good snow thickness and density outcome although the model somewhat underestimates the total compaction rate (Fig. 7). Also because of this artificial regularity there were no peaks in model snow thickness and all formed slush was frozen soon into snow-ice. In reality persistent slush layers have been found also on the Kleye Strait ice. Observations of the bulk density of ice gave values less than 0.9 Mg/m^3 on 12 February and 0.85 Mg/m^3 at the lowest, which indicates the existence of relatively porous ice such as snow-ice. The sensitivity of the model ice thickness to the

oceanic heat flux was large: the low level of 5 W/m^2 resulted in the ice thickness of 102 cm, while the high level of 20 W/m^2 gave the ice thickness of only 67 cm.

The long-term (1987–1996) simulations were performed using the NCEP/NCAR reanalysis data, which result from a state-of-the-art analysis/forecast system to perform data assimilation using past data from 1958 to the present. A large subset of the data is available from NOAA-CIRES Climate Diagnostic Center in its original four times daily format. Here the thermal forcing at the surface and precipitation are needed, and they are directly provided in the reanalysis data as the fluxes of net long-wave radiation, net short-wave radiation, latent heat and sensible heat, and precipitation rate. The grid size is about 200 km in the Okhotsk Sea region, and the point closest to Kleye Strait was selected for the 10-year simulations, located inland Sakhalin. The starting time of the model was chosen as the date when the surface temperature fell below –2^{o}C in the NCEP data.

A comparison between this simulation with the individual ice season 1994/95 is presented in Fig. 8. The agreement is worse than when using the local weather data. The ice thickness is biased up by 20 cm while the snow thickness is rather good for the total volume but timing is biased. However, in the absence of long-term local weather record, the correspondence is still considered acceptable to produce ice climatology. The main reason for the ice thickness being biased up is that the air temperature must be lower in inner Sakhalin than on the coast.

The results of the 10-year-mean evolution are shown in Fig. 9. The site freezes on 5 November and the breakup of ice takes place on 5 June. Comparing with the long-term averages, the breakup date is close (12 June) but the freezing date is well ahead (25 November). The maximum annual ice thickness becomes 108 cm, and the ice sheet consists of 70 cm of congelation ice and 38 cm of snow-ice. The snow thickness reaches the maximum of 30 cm in February. The mean thicknesses of ice and snow correspond rather well to the observation statistics (Table 2) except that the timing of the snow peak is earlier in the model outcome and (probably because of that) the spring snow-ice growth does not come out very well.

5. Conclusions

The thickness of coastal fast sea ice in the Sea of Okhotsk has been examined based on field data and thermodynamic modelling. The study sites were Saroma-ko Lagoon, Hokkaido and Kleye Strait, Sakhalin. They represent the ice conditions in the southern and northern parts of the Sea of Okhotsk. The following conclusions are made on the field observations:

1. In Saroma-ko Lagoon, the freezing and breakup dates are 8 January ± 7 days and 12 April ± 6 days (here and below ± is for the standard deviation). The ice grows to 34 ± 13 cm in mid-February to 8 cm more thereafter. The ice sheet has a two-layer structure: granular snow-ice layer on top and columnar ice layer below. The proportions of the layers vary widely, at extrema all ice may consist of snow-ice or 90% may consist of congelation ice.

2. In Kleye Strait, the ice grows to 39 ± 10 cm in December, 54 ± 9 cm in January, 71 ± 11 cm in February, 76 ± 12 cm in March, and 100 ± 7 cm in April. The ice sheet has a two-layer structure: granular snow-ice layer on top and columnar ice layer below. A remarkable addition to ice thickness, on average 24 cm (from 76 to 100 cm thickness) results during mid-March to mid-April due to snow-ice formation.

A one-dimensional thermodynamic model was calibrated with observed data and used to examine the thickness climatology. The model consists of Maykut and Untersteiner (1971) type congelation ice treatment and a snow model, which takes account of snow compaction, slush formation, and snow-ice growth. The model was forced by observed weather records for the air – ice/snow heat exchange and precipitation; the oceanic heat flux was kept constant in one model simulation. Validation was made against observed snow and ice thickness. The model outcome showed reasonably good agreement for both sites. The following conclusions are made from the model simulations:

3. In Saroma-ko Lagoon the calibration was based in four winters. The maximum annual ice thickness was 3 cm biased down on average, 16 cm in the worst case; the model snow thickness was within 10 cm from the observed in February; and the date of ice breakup was on average biased late by 5 days, 11 days in the worst case. The large year-to-year variability of the snow-ice and congelation ice layers corresponds well to recent

observations in the Saroma-ko Lagoon. The model simulations gave a prediction of the formation of slush layers and their persistency for 1–4 weeks in different winters. Climatological simulation resulted in mean maximum annual ice thickness of 32 cm, of which 15 cm was snow-ice, and ice breakup on 20 April.

4. In Kleye Strait the calibration was based on one ice season. The maximum annual ice thickness was 7 cm biased down, and the model snow thickness was within 10 cm from the observed level. The ice grows as congelation ice until around mid-February, and then the snow-ice formation begins. Climatological simulation by using the NCEP/NCAR data resulted in mean maximum annual ice thickness of 108 cm, of which 70 cm was congelation ice and 38 cm was snow-ice, and ice season lasted through 5 November to 5 June. Problems in the model outcome are partly due to the NCEP/NCAR data not being very well representative for local weather; the freezing date was biased earlier by 20 days and the maximum annual ice thickness by 10–20 cm.

The main outcome of the paper is in the role of snow and slush in the growth and melting of sea ice based on data and modelling. The timing of the snowfall largely influences the snow-ice growth, slush controls the temperature conditions and may persist several weeks, oceanic heat flux may eat congelation ice and give more space for snow-ice growth, and the spring snow-ice growth due to daily melt–freeze cycles may be highly significant.

The field programme continues in Kleye Strait for a good long-term database for the landfast sea ice and its thermal forcing. In Saroma-ko Lagoon a detail experimental study is ongoing to examine the snow-slush-snow ice process including the evolution of the salinity distribution (Kawamura et al., 2004). These data not only provide real information on ice structure but also will tell where and how errors come into model simulations. In the modelling development salinity and mechanical breakage of ice needs to be included. The evolution of the landfast ice will aid also basin wide models of the ice conditions in the Sea of Okhotsk by providing excellent control for the thermodynamics.

Acknowledgments. We wish to thank the Saroma Research Center of Aquaculture in Sakaeura and Chaivo Research Station, Sakhalin Oil and Gas Research Institute for their kind

offers to use their facilities and assistance in the field, and also Eriko Uematsu for drafting. This work is a part of the project "Ice Climatology in the Okhotsk and Baltic Seas" financed by the Japanese-Finnish Bilateral Programs for Scientist Exchange with the Japan Society for the Promotion of Science, the Academy of Finland, and the Sea Ice Research Laboratory's Overseas Fieldwork Program (Monbusho); this work is also a part of the project "An Experimental Study for Modelling of Air-Sea-Ice-Ecosystem in Seasonal Sea-Ice Evolution" financed by the Japanese Ministry of Education, Science and Culture (Monbusho) through grants-in-aid for Scientific Research, and the Sasakawa Scientific Research Grant from the Japan Science Society. NCEP/NCAR Reanalysis data were provided through the NOAA Climate Diagnostics Center (http://www.cdc.noaa.gov/) for the long-term model simulations.

6. References

Anon., 2000. The 2nd Ice Scour & Arctic Marine Pipelines Workshop. In *Proceedings of the 15th International Symposium on Okhotsk Sea & Sea Ice*, 260 p. Mombetsu, Hokkaido, Japan.

Aota, M., Ishikawa, M., Murai, K. and Hirata, T., 1993. Variation of accumulated ice concentration off Abashiri, Okhotsk Sea coast of Hokkaido (in Japanese). *Uminokenkyu,* 2: 251–260.

Crocker, G. B. and P. Wadhams, P., 1989. Modelling Antarctic fast-ice growth. *Journal of Glaciology,* 35: 3–8.

Fritsen, C.H., Ackley, S.F., Kremer, J.N., Sullivan, C.W., 1998. Flood-freeze cycles and microalgal dynamics in Antarctic pack ice. *Antarctic Research Series* 73: 1–21. American Geophysical Union.

Fukutomi, T., 1950. Study of sea-ice (The 4th Report). A theoretical study on the formation of sea-ice in the central part of the Okhotsk Sea (in Japanese with English summary). *Low Temperature Science, Ser. A,* 3: 143–157.

Fukutomi, T., 1952. Study of sea-ice (The 17th Report). On the maximum thickness of winter ice at northern seacoasts (in Japanese with English summary). *Low Temperature Science, Ser. A,* 9: 125–136.

Kawamura, T., Shirasawa, K., Ishikawa, M., Takatsuka, T., Daibou, T. and Leppäranta, M., 2004. On the annual variation of characteristics of snow and ice in Lake Saroma. *Proeedings of the 17th IAHR Ice Symposium*, Vol. 1, pp. 211-220. St. Petersburg, Russia.

Leppäranta, M., 1983. A growth model for black ice, snow ice and snow thickness in subarctic basins. *Nordic Hydrology,* 14(2): 59–70.

Leppäranta, M., 1993. A review of analytical sea ice growth models. *Atmosphere–Ocean,* 31: 123–138.

Leppäranta, M. and Kosloff, P., 2000. The structure and thickness of Lake Pääjärvi ice. *Geophysica,* 36(1-2): 233–248.

Leppäranta, M., K. Shirasawa and Saloranta, T., 1997. On the oceanic heat flux and sea ice thickness. *Proceedings of the 12th International Symposium on Okhotsk Sea & Sea Ice, 2–5 February 1997, Mombetsu, Japan*, pp. 154–159.

Lytle, V.I. and Ackley, S.F., 2001. Snow-ice growth: a fresh-water flux inhibiting deep convection in the Weddell Sea, Antarctica. *Annals of Glaciology 33: 45–*50.

Maksym, T. and Jeffries, M.O., 2000. A one-dimensional percolation model of flooding and snow ice formation on Antarctic sea ice. *Journal of Geophysical Research, 105(C11):* 26,313–26,331.

Maykut, G.A. and Untersteiner, N., 1971. Some results from a time-dependent, thermodynamic model of sea ice. *Journal of Geophysical Res.earch,* 76: 1550–1575.

Omstedt, A., 1990. A coupled one-dimensional sea ice-ocean model applied to a semi-enclosed basin. *Tellus,* 42A: 568–582.

Palosuo, E., 1965. Frozen slush on lake ice. *Geophysica,* 9: 131–147.

Peixoto, J.P. and Oort, A.H., 1992. *Physics of Climate*. American Institute of Physics.

Perovich, D.K., 1998. The optical properties of sea ice. In *Physics of Ice-covered Seas*, edited by M. Leppäranta, Helsinki University Printing House, pp. 195–230.

Polomoshnov, A., 1992. Seasonal variability of sea ice physico-mechanical properties. *Proceedings of the7th International Symposium on Okhotsk Sea & Sea Ice, pp. 336-339,* Mombetsu, Japan.

Polomoshnov, A., 1994. Hydrologic regime in Chaivo Bay. *Proceedings of the 9th International Symposium on Okhotsk Sea & Sea Ice,* pp. 147–149, Mombetsu, Japan.

Reed, R.K., 1977. On estimation insolation over the ocean. *Journal of Physical Oceanography,* **7**, 482–485.

Saloranta, T., 1998. Snow and snow ice in sea ice thermodynamic modelling. *Report Series in Geophysics,* University of Helsinki, No. 39, 84 pp.

Saloranta, T., 2000. Modeling the evolution of snow, snow ice and ice in the Baltic Sea, *Tellus,* 52A: 93–108.

Sapporo District Meteorological Observatory, 1996. *Monthly Hokkaido Meteorological Data Report, January 1987 to December 1996*.

Shimoda, H., Uto, S., Tamura, K. and Narita, S., 1996. Sea ice situations in the Sea of Okhotsk off the coast of Hokkaido by on board ship observations (in Japanese with English summary). *Proc. 11th Intl. Symp. Okhotsk Sea & Sea Ice,* pp. 156-160*, Mombetsu, Japan*.

Shirasawa, K., 1998. Sea ice in the Okhotsk Sea –Effects by global warming ? (in Japanese). In *Hydrology and Water Resources in Snow-Covered Regions,* ed. by the Japan Soc. Hydrol. & Water Resour. Editorial Board, p. 191–204, Shinzansha Scitech, Tokyo.

Shirasawa, K. and Leppäranta, M., 1996. Comparisons between the Okhotsk Sea and the Baltic Sea ice, *Proc. 11th Intl. Symp. Okhotsk Sea & Sea Ice*, pp. 215-227, Mombetsu, Japan.

Shirasawa, K., Ikeda, M., Ishikawa, M., Takatsuka, T., Kodama, Y., Aota, M., Takahashi, S., Takizawa, T., Polomoshnov, A., Truskov, P. and Astafiev, V., 1996a. Meteorological data report for the sea ice studies at Val, Chaivo and Kleye Strait, northern Sakhalin. *Low Temp. Sci., Ser. A., 55, Data Report*, 137–229.

Shirasawa, K., Ikeda, M., Ishikawa, M. Takatsuka, T. Aota, M. and Fujiyoshi, Y., 1996b. Sea ice conditions and meteorological observations at Saroma-ko lagoon, Hokkaido, December 1995 - November 1996. *Low Temp. Sci., Ser. A., 55, Data Report*, 47–77.

Shirasawa, K., Ingram, R.G. and Hudier, E., J-J., 1997. Oceanic heat fluxes under thin sea ice in Saroma-ko lagoon. Hokkaido, Japan, *J. Marine Systems,* 11: 9–19.

Shirasawa, K., Leppäranta, M. and Saloranta, T., 1998. Interannual variability in sea ice of Saroma-ko Lagoon, Hokkaido, Japan. *Proc. 2nd International Conference on Climate and Water, Espoo, Finland,* vol. 3, pp. 1147–1156.

Shirasawa, K., Saloranta, T. and Leppäranta, M., 2000. On the modeling of the thickness climatology for the coastal ice in the Sea of Okhotsk. *Proc. 15th Intl. Symp. Okhotsk Sea & Sea Ice,* pp. 121–127, *Mombetsu, Japan*.

Stefan, J., 1891. Über die Theorie der Eisbildung, insbesondere über Eisbildung im Polarmeere, *Ann. Physik, 3rd Ser.*, 42: 269–286.

Tabata, T., Nohguchi, Y. and Saito, T., 1980. Observed sea ice thickness in the northern Okhotsk Sea (in Japanese with English summary). *Low Temperature Science, Ser. A,* 39*:* 153–158.

Talley, L. D. and Nagata, Y., 1995. The Okhotsk Sea and Oyashio region (Report of Working Group 1). *PICES Scientific Report No. 2*, 227 p.

Yen, Y.-C., 1981. Review of thermal properties of snow, ice and sea ice. *CRREL Report* 81-10: 1–27.

Zubov, N.N., 1945. *L'dy Arktiki* [Arctic Ice]. Izdatel'stvo Glavsermorputi, Moscow. Engl. transl. 1963 by U.S. Naval Oceanogr. Office and Amer. Meteorol. Soc., San Diego.

Table 1. Ice climatology for the Saroma-ko lagoon off Hokkaido (1992–1996). 15 February and Maximum columns show thicknesses in cm.

	Freezing	15 February		Maximum	Full Ice Coverage	
	Day	Ice	Snow	Ice	Formation	Breakup
Average	8 January	34.2	11.0	42.3	3 February	12 April
St.dev.	7 days	12.9	10.1	7.1	2 days	6 days

Table 2. Ice and snow thickness climatology (cm) for the Chaivo Station, Kleye Strait off Sakhalin (1990–1995); x = no data.

	15 December		15 January		15 February		15 March		15 April	
	Ice	Snow	Ice	Snow	Ice	Snow	Ice	Snow	Ice	Snow
Average	38.5	7.7	54.3	6.8	70.7	20.3	76.0	21.7	99.7	x
St. Dev	9.8	5.5	8.8	2.8	10.9	9.8	11.8	11.7	6.7	x

Table 3. The standard model parameters and constants.

Ice density	$\rho_i = 0.91$ Mg/m^3	
Snow-ice density	$\rho_{si} = 0.875$ Mg/m^3	Palosuo (1965)
New snow density	$\rho_{so} = 0.225–0.25$ Mg/m^3	
Slush density	$\rho_i = 0.92$ Mg/m^3	
Thermal conductivity of ice	$\kappa_i = 2.09$ W m^{-1} $^oC^{-1}$	Yen (1981)
Thermal conductivity of snow-ice	$\kappa_{si} = \kappa_i/2$	
Specific heat of ice	$c_i = 2.114$ kJ kg^{-1} $^oC^{-1}$	Yen (1981)
Latent heat of freezing	$L = 333.5$ kJ/kg	Yen (1981)
Albedo, dry snow and ice	$\alpha = 0.87$, $\alpha = 0.7$	Perovich (1998)
Albedo, melting snow and ice	$\alpha = 0.77$, $\alpha = 0.3$	Perovich (1998)
Surface emissivity	$\varepsilon = 0.97$	Omstedt (1990)
Grid size	10 cm (ice), 3 cm (snow)	

Table 4. The maximum annual ice thickness and ice breakup date in the Saroma-ko Lagoon according to the model and observations.

Year	Maximum ice thickness		Ice breakup date	
	Model	Observed	Model	Observed
1992	26	42	6 April	4 April
1994	45	40	21 April	17 April
1995	45	52	12 April	10 April
1996	39	35	27 April	16 April
Mean	39	42	17 April	12 April

Figure captions

Figure 1. Isopleths showing the estimated mean annual maximum ice thickness in the Sea of Okhotsk (Fukutomi, 1950). The numbers in brackets [·] indicate observed maximum ice thicknesses from Fukutomi (1952) and Tabata et al. (1980). Also shown are (a) the site location in Kleye Strait, and (b) the site location in Saroma-ko Lagoon. The line in Saroma-ko Lagoon indicates the snow/ice survey line.

Figure 2. A schematic illustration of the model layers.

Figure 3. The model outcome of the thicknesses of congelation ice, snow-ice and snow for Saroma-ko Lagoon, 1992 and 1994–1996, shown together with observations.

Figure 4. The mean evolution of ice thickness in Saroma-ko Lagoon according to the model runs. The oceanic heat flux is 5 W/m^2.

Figure 5. The mean evolution of ice and snow thickness in Saroma-ko Lagoon according to the model runs for the oceanic heat fluxes of (a) $Q_w = 0$ and (b) $Q_w = 20$ W/m^2.

Figure 6. Seven-year average a) slush thickness and b) bulk snow density at Saroma-ko Lagoon according to the model simulations.

Figure 7. The model calibration for the Kleye Strait, ice season 1994/1995: (a) Modelled (ice; dark shaded, snow ice; medium shaded, snow; light shaded) and observed (- + - +) total ice and snow thickness; (b) Modelled and observed bulk density of snow, (c) Modelled and observed ice-snow interface temperature.

Fig. 8. Model outcome against observations in Kleye Strait when forcing the model with NCEP/NCAR data, ice season 1994/1995.

Figure 9. Ten-year mean evolution of ice and snow thickness Kleye Strait according to the model simulations.

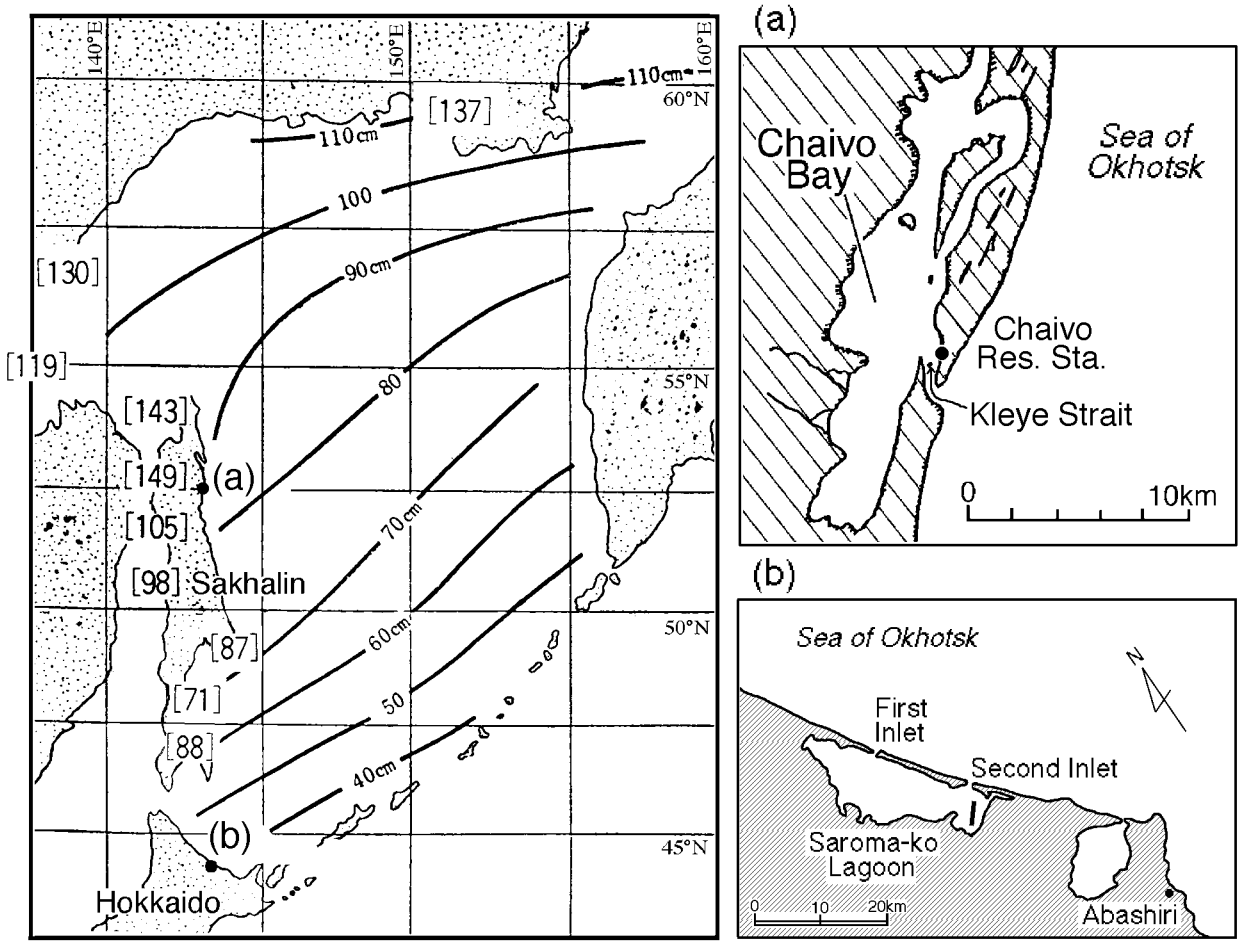

Fig.1 Isoplethes showing the estimated mean annual maximum ice thickness in the Sea of Okhotsk [Fukutomi, 1950]. The numbers in brackets [·] indicate observed maximum ice thicknesses from Fukutomi [1952] and Tabata et al. [1980]. Also shown are (a) the site location in Kleye Strait and (b) the site location in Saroma-ko Lagoon. The line in Saroma-ko Lagoon indicates the snow/ice survey line.

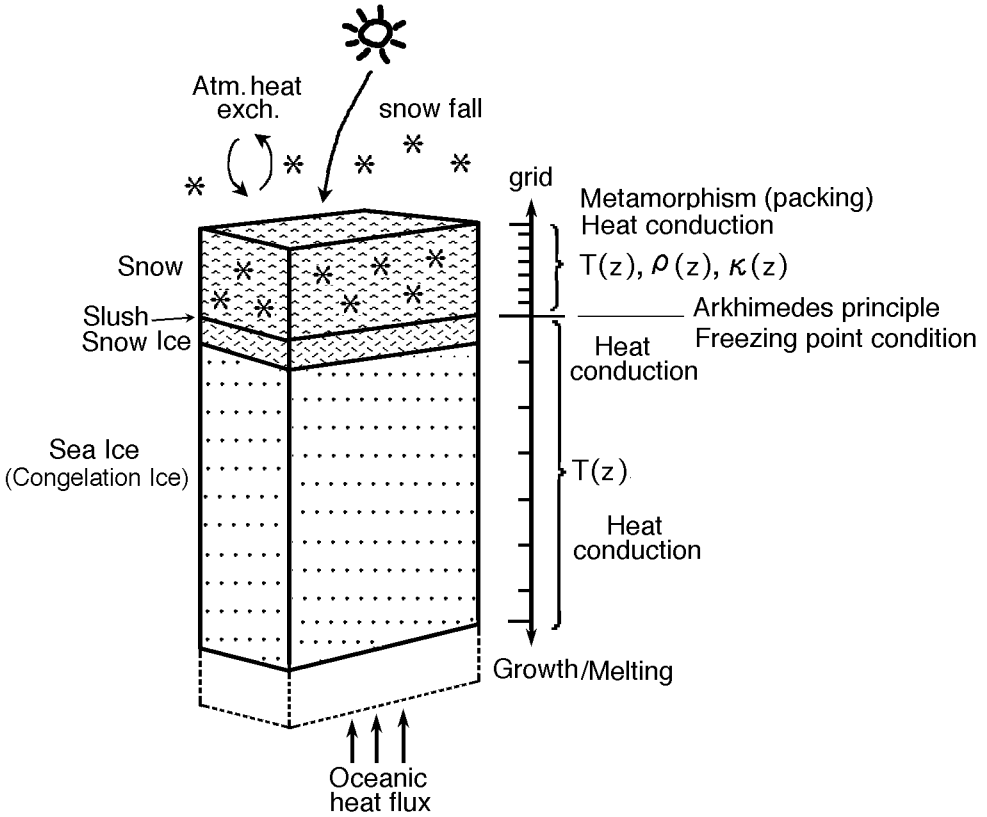

Fig.2 A schematic illustration of the model layers.

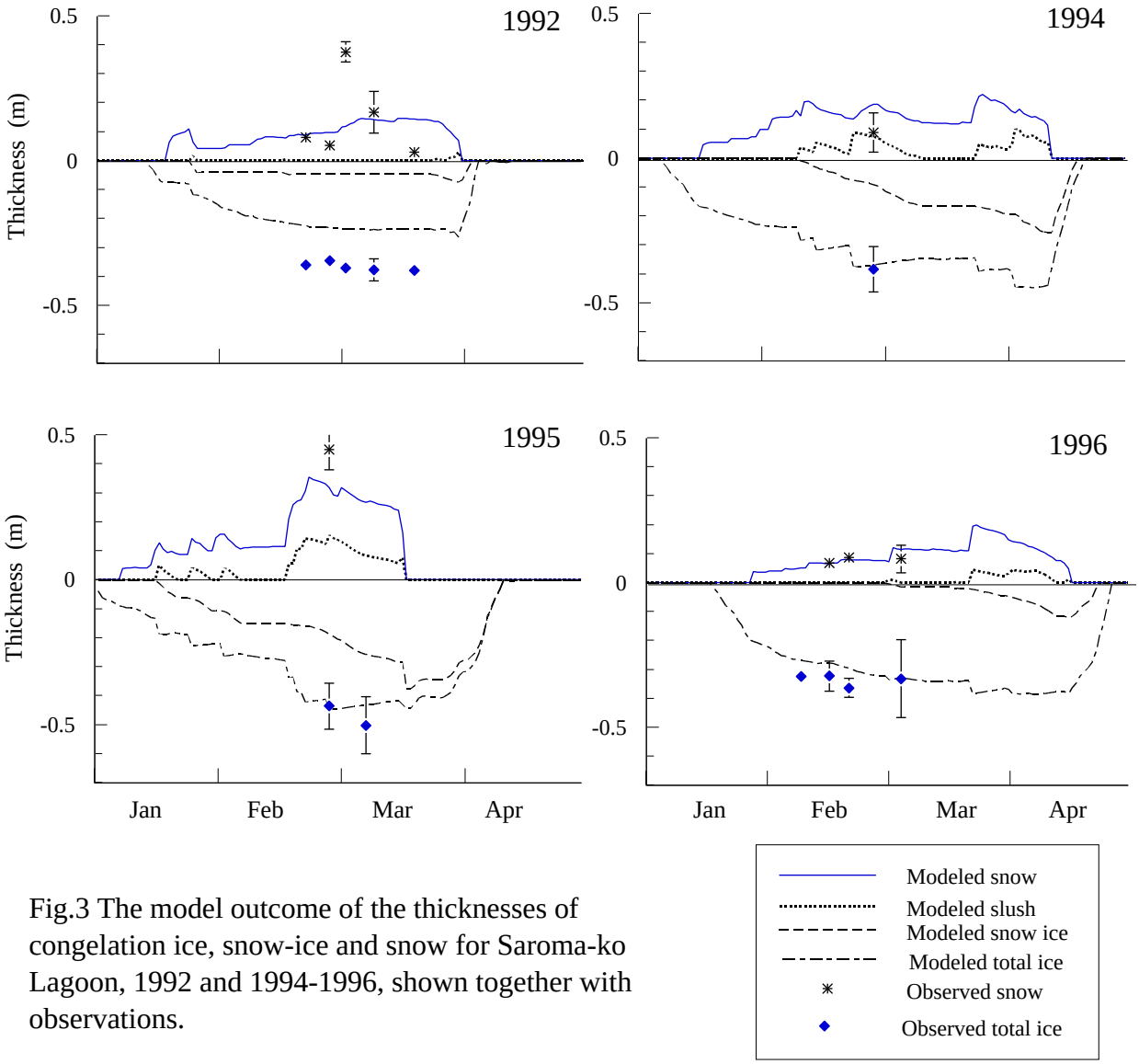

Fig.3 The model outcome of the thicknesses of congelation ice, snow-ice and snow for Saroma-ko Lagoon, 1992 and 1994-1996, shown together with observations.

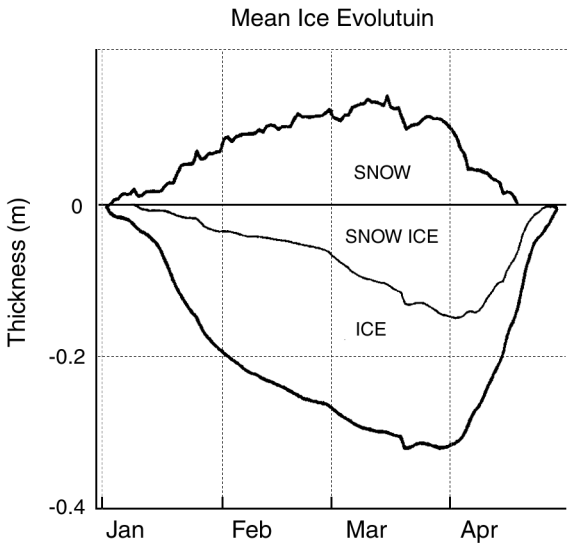

Fig.4 The mean evolution of ice thickness in Saroma-ko Lagoon according to the model runs. The oceanic heat flux is 5W/m^2.

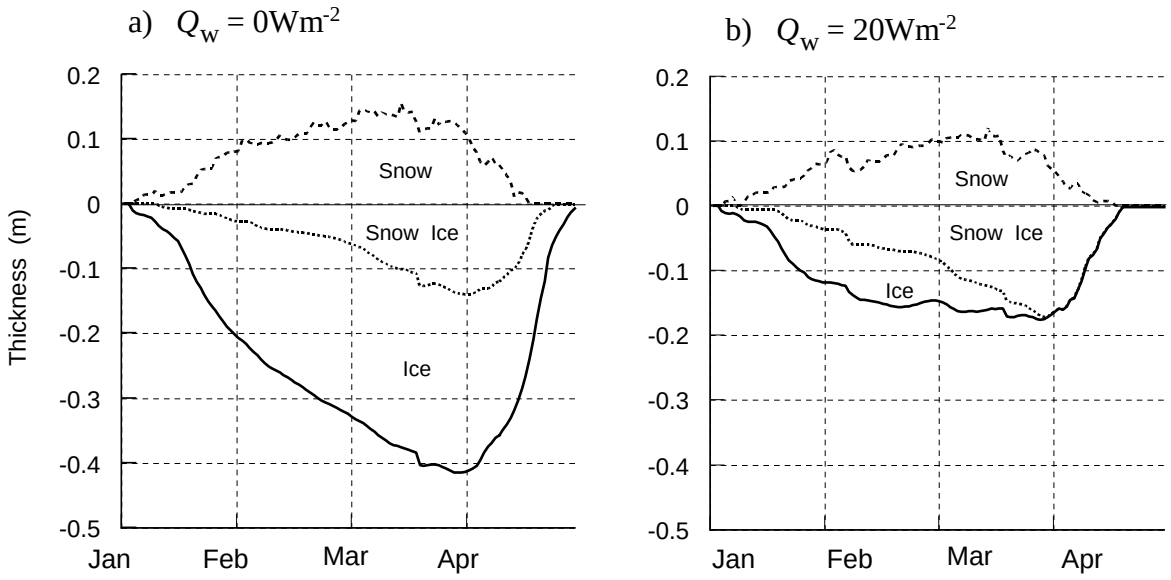

Fig. 5 The mean evolution of ice and snow thickness in Saroma-ko Lagoon according to the model runs for the oceanic heat fluxes of (a)Q_w=0 and (b) Q_w=20 W/m^{-2} .

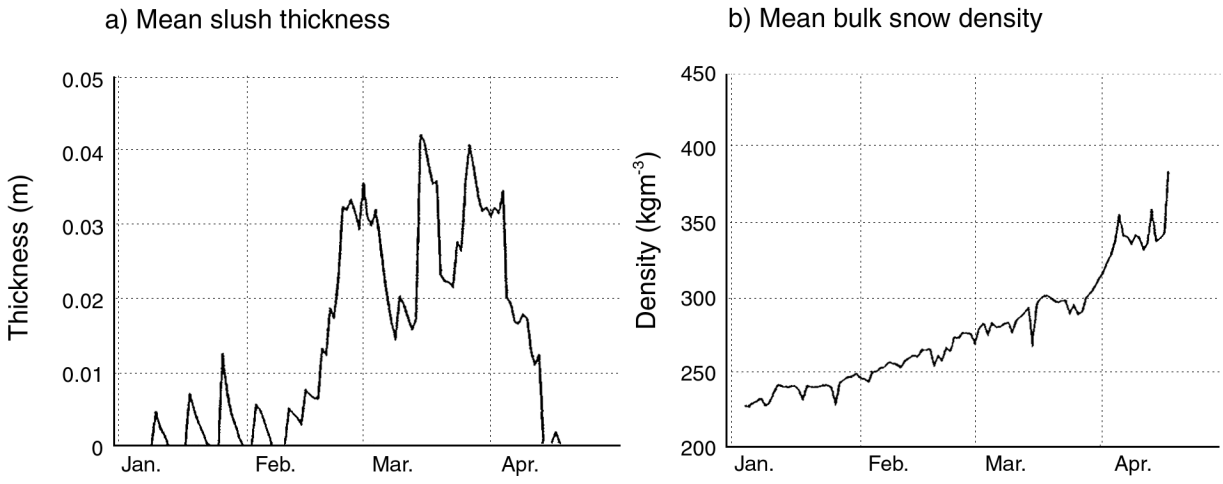

Fig.6 Seven-year average a) slush thickness and b) bulk snow density at Saroma-ko Lagoon according to the model simulations.

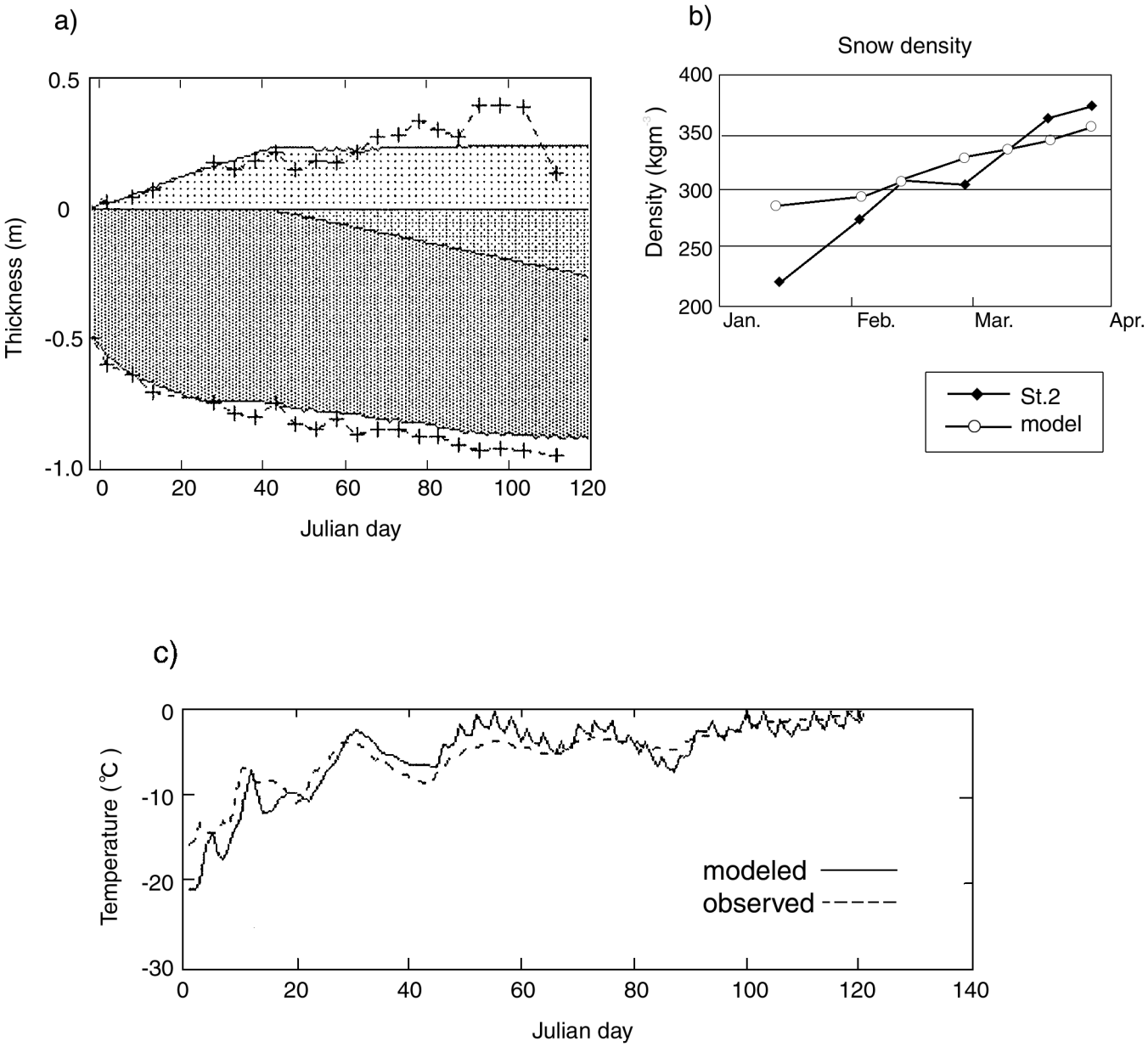

Fig. 7 The model calibration for the Kleye Strait, ice season 1994/1995: (a) Modelled (ice; dark shaded, snow ice; medium shaded, snow; light shaded) and observed (- + - +) total ice and snow thickness; (b) Modelled and observed bulk density of snow, (c) Modelled and observed ice-snow interface temperature.

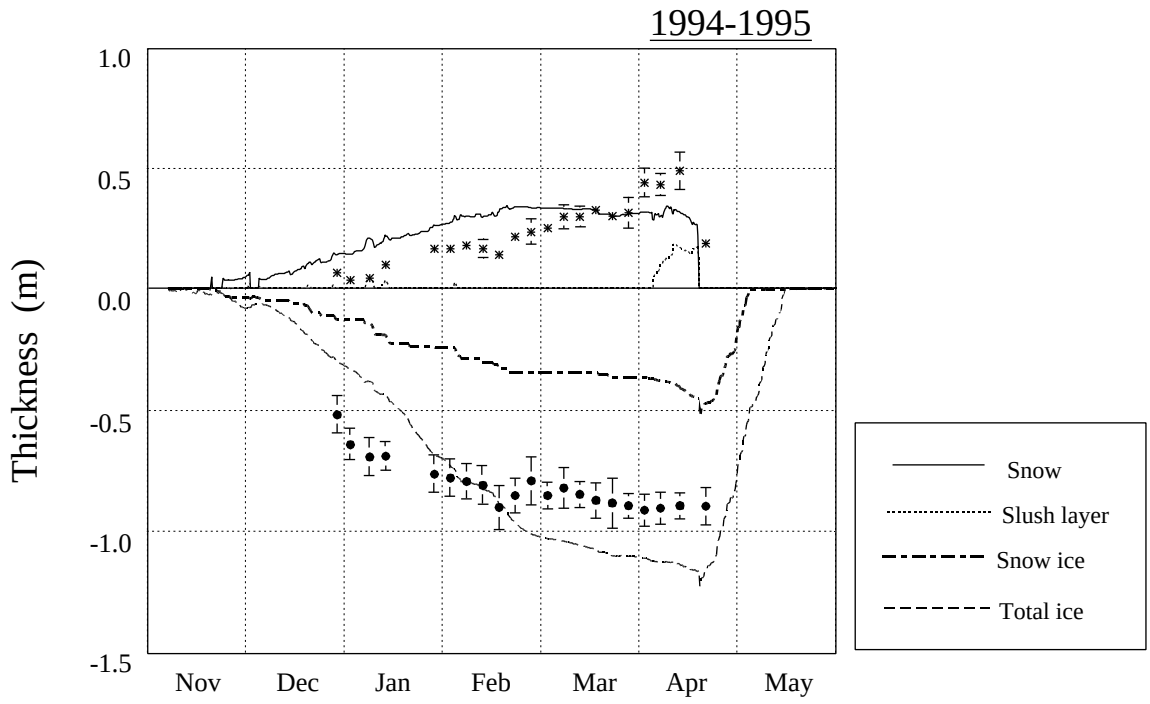

Fig. 8 Model outcome against observations in Kleye Strait when forcing the model with NCEP/NCAR data, ice season 1994/1995.

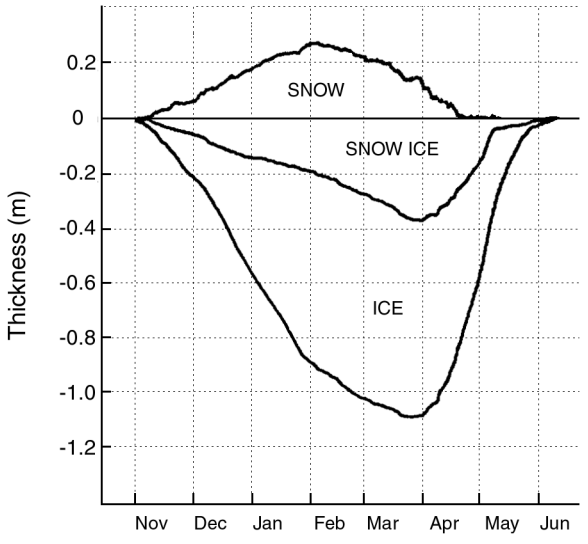

Fig.9 Ten-year mean evolution of ice and snow thickness at Kleye Strait according to the model simulations.